JOC The Journal of Organic Chemistry

Article

Computational insight into 1,2-diamine, -diether, and -amino ether chiral ligands-mediated carbolithiation: a case of enantioinduction reversal

Hélène Guyon, Anne-Sophie Castanet, and Anne Boussonnière

J. Org. Chem., **Just Accepted Manuscript** • DOI: 10.1021/acs.joc.0c00832 • Publication Date (Web): 29 Jun 2020

Computational insight into 1,2-diamine, -diether, and -amino ether chiral ligands-mediated carbolithiation: A case of enantioinduction reversal

Hélène Guyon, Anne-Sophie Castanet,* and Anne Boussonnière*

Institut des Molécules et Matériaux du Mans (IMMM) - UMR 6283 CNRS - Le Mans Université,

Avenue Olivier Messiaen, 72085 Le Mans, France

anne.boussonniere@univ-lemans.fr, anne-sophie.castanet@univ-lemans.fr

Table of contents

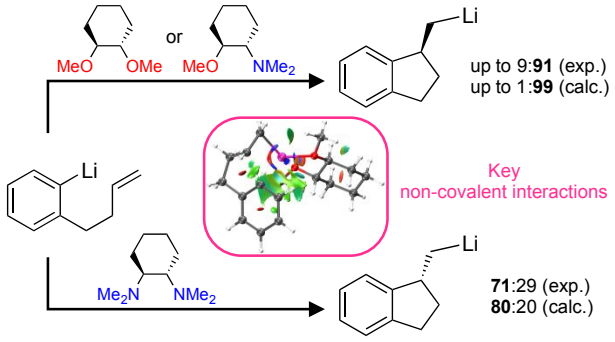

ABSTRACT. *trans*-1,2-cyclohexanediamine, -diether and -amino ether were compared as chiral inducers in the asymmetric intramolecular carbolithiation of olefinic aryllithiums. Switching from diamine to ethereal ligands inverts the sense of asymmetric induction. This reversal of stereoselectivity was investigated through DFT calculations. High enantioselectivities observed with diether and amino ether ligands arise from favorable weak interactions between the ligand and the substrate. The relative efficiency of the three ligands and sense of stereoinduction for the most efficient diether and amino ether ligands prove to be foreseeable by modeling the reaction with the parent achiral 1,2-bidentate additives and comparing the diastereomeric transition states stemming from the two half-chair conformations of their lithium chelate.

Introduction

Bidentate Lewis donor bases, such as 1,2-diamines and diethers, are known to alter organolithiums reactivity, notably by reshaping their aggregation state in solution.[1] This ability has long been exploited to achieve asymmetric reactions by using (−)-sparteine in association with organolithiums.[2] Major progress in this field has also been achieved by the design of C_2-symmetric diamine or diether ligands, e.g. **L1** and **L2**, as efficient chiral inducers (Figure 1).[3,4]

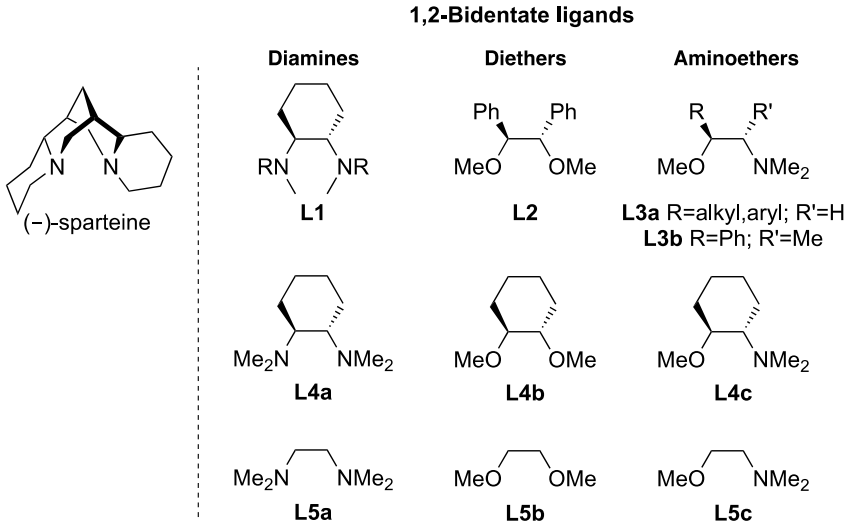

Figure 1. Examples of bidentate Lewis donor bases

We recently described an alternative novel class of ligands, natural amino acid-derived 1,2-amino ethers **L3a**, which at least equals and often outperforms the above-mentioned ligands in asymmetric intramolecular carbolithiation.[5,6]

To date, identification of an effective chiral ligand still relies on a trial-and-error approach, mostly by modifying its chiral carbon backbone. As a consequence, the key structural features of the ligands, responsible for achieving high stereoselectivity, are not clearly identified and understood. In particular, there remains the intriguing question of the impact of the Lewis basic chelating functional groups of the ligand (diamine, diether, amino ether) on the stereoselectivity of the reaction. Indeed, little information on this particular point can be found in the literature (Scheme 1).

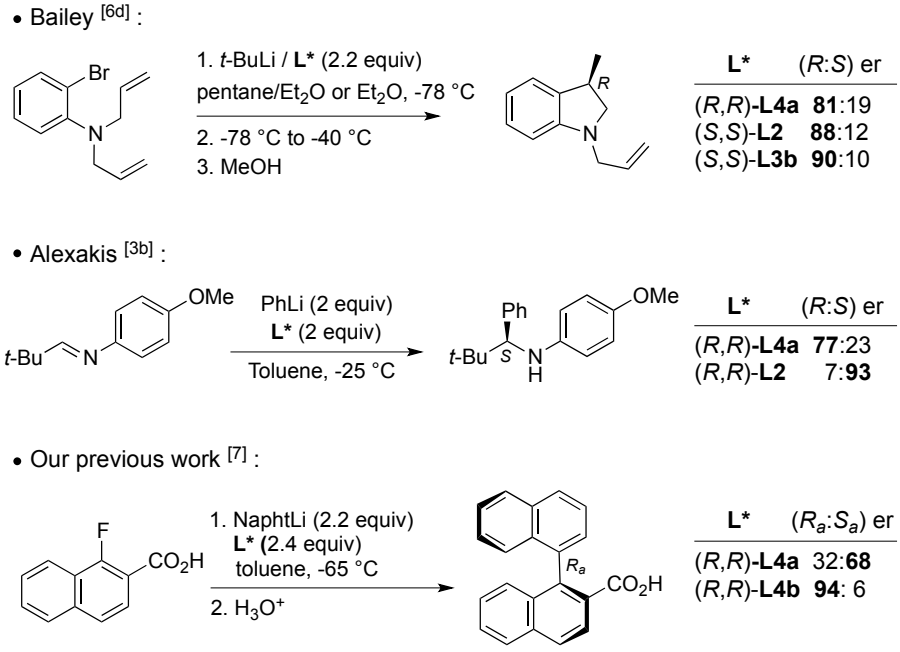

Scheme 1. Comparison of chiral diamines, diethers and amino ethers as chiral ligands in literature

During an extensive screening of chiral ligands in enantioselective intramolecular carbolithiation - one of the scarce study including amino ether ligands - Bailey observed that diamine (*R*,*R*)-**L4a** leads to the same major enantiomer as both the diether (*S*,*S*)-**L2** and amino ether (*S*,*S*)-**L3b**. [6d] In their report on asymmetric 1,2-addition of aryllithium to imines, Alexakis and al. described an enantioreversal between a 1,2-diamine and a 1,2-diether despite of the same chirality of the ligand scaffolds. [3b] However, from a rigorous point of view, the differences in the carbon backbone of the ligands compared in these two studies prevents any formal conclusion on the impact of the chelating groups. More conclusive results can be found from our study on atroposelective S_NAr reaction, since a reversal in product chirality was observed by switching from cyclohexanediamine (*R*,*R*)-**L4a** to parent diether (*R*,*R*)-**L4b**. [7]

Taken together, all the above results strongly suggest that the observed enantioreversal is not an accidental phenomenon limited to S_NAr but might be rather general when organolithium reagents are used as nucleophiles. To further probe this assumption, we decided to formally compare diamine, diether and aminoether ligands (*S*,*S*)-**L4a-c** (Figure 1) in the same enantioselective reaction. Our objective was not restricted to experimental results but more importantly we aimed at a better understanding of the underlying factors responsible for the stereoinduction through DFT studies, as this information could help further rational design of chiral ligands. Toward that goal, we selected the intramolecular carbolithiation reaction as our model reaction, guided by our interest for this

transformation[5] and inspired by recent mechanistic studies on "racemic" carbolithiation[8a-b]. In this article, we report the first computational study elucidating the origin of the enantioinduction reversal observed when switching from 1,2-diamine to 1,2-ethereal ligands in intramolecular carbolithiation.

Computational methods

PM6 semi-empirical conformational analyses were conducted with Spartan 14. Geometry optimizations and IRC analysis were performed with the help of Gaussian 16 package in gas-phase at 298 K, employing DFT functional B3LYP-D3/6-31+G(d), including dispersion corrections by means of Grimme's D3 model. [9] All the optimized geometries were submitted to single point energy calculation and vibrational analysis at the B3LYP-D3/6-311+G(d,p) level using polarizable continuum model (PCM) for implicit solvation with toluene. QTAIM analyses were carried out by using AIMAll package (Version 15.09.27).[10] The NCI analyses were conducted with the help of Multiwfn[11] and visualized using VMD. [12]

Results and Discussion

Experimental results

To understand the influence of the amino versus the ether function of the chiral ligand on a carbolithiation stereochemical course, we investigated a series of three 1,2-bidentate ligands: C_2-symmetric diamine and diether **L4a** and **L4b** and pseudo-C_2-symmetric amino ether **L4c**.

To ensure that the trends in stereoselectivities are not substrate-dependent, two different substrates, **1a** and **1b,** were evaluated in the **L4**-mediated enantioselective intramolecular carbolithiation (Scheme 2).

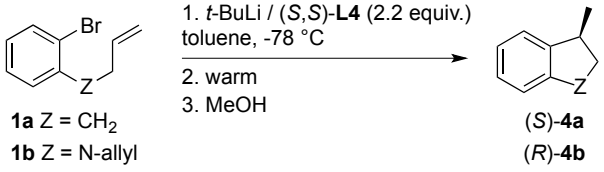

	4a (*R*:*S*) er	4b (*S*:*R*) er
L4a	**71**:29	**79**:21
L4b	9:**91**	12:**88**
L4c	15:**85**	8:**92**

Scheme 2. Evaluation of ligands **L4a-c** in the intramolecular carbolithiation of substrates **1a** and **1b**.

Aryl bromides **1a** and **1b** were submitted to lithium-bromide exchange at -78 °C in toluene with 2.2 equiv. of the preformed *t*-BuLi/chiral ligand complex. The resulting aryllithiums were warmed respectively to room temperature and -40 °C to achieve the cyclization, then methanolized.[13] The enantiomeric ratios were determined by chiral stationary phase GC analysis. The highest stereoselectivities were obtained with either diether **L4b** (9:91 e.r. from **1a**) or amino ether **L4c** (8:92 e.r. from **1b**). In the field of chiral ligand-mediated synthesis, C_2-symmetric chiral

inducers have long been favored. As their element of symmetry reduces the number of diastereomeric pathways of a reaction, they were believed to consistently lead to the best level of stereoinduction.[14] This assumption has restrained the design of C_1-symmetric ligands, but numerous studies support now the relevance of such non-symmetric chiral additives.[15] The good levels of enantioinduction obtained with amino ether **L4c** further demonstrate the potential of C_1-symmetric ligands. Furthermore, as anticipated, a distinct reversal of stereoselectivity was observed on both substrates between the ethereal ligands and diamine **L4a**, confirming that the nature of the chelating functions affects not only the level of enantioselectivity but also its sense. In an effort to rationalize these intriguing experimental results, we engaged in a computational study of the stereochemical course of the bidentate ligand-mediated intramolecular carbolithiation of **1a**.

Earlier theoretical studies support a carbolithiation mechanism involving a lithium-alkene coordination, prior to the intramolecular addition of the organolithium across the double bond.[8] This coordination would take place upon disaggregation of an oligomeric form of the aryllithium toward a monomeric complex. Thus, we assumed the formation of complex **2a**, preceding the carbolithiation, with a tetracoordination around the lithium atom, bound to the double bond, the anionic carbon on the aromatic ring, and the bidentate Lewis donor base (Scheme 3).

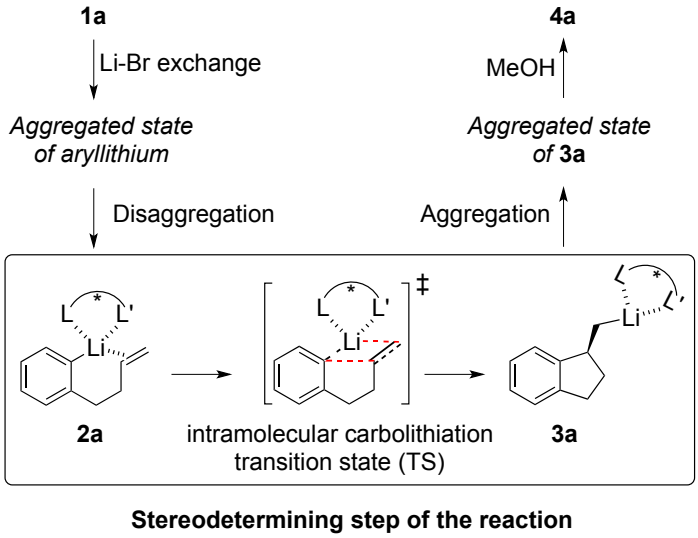

Scheme 3. Global carbolithiation process from bromoarene **1a** to indane **4a**

Once the cyclization is achieved via a four-center transition state, the resulting organolithium **3a** likely evolves towards a more stable aggregated state with tetracoordinated lithium atoms. Our focus being on the

stereochemical course of the carbolithiation, the following study aims at modeling the stereodetermining step of the reaction (**2a** → TS → **3a**).

To validate the model, the computation was first carried out on the carbolithiation reaction mediated by achiral bidentate additives **L5a-c** (Figure 1).[16]

Achiral 1,2-bidentate ligands

For each ligand a similar approach was carried out to investigate the reaction pathway[17]: a semi-empirical conformational analysis of the precomplexes **2a** was conducted followed by elucidation of the corresponding transition states ($TS_{\mathbf{2a\text{-}3a}}$) at the B3LYP-D3/6-31+G(d) DFT level in gas-phase at 298 K. For each resolved TS, an Intrinsic Reaction Coordinate (IRC) analysis was conducted and the corresponding precomplex **2a** and final product-ligand complex **3a** geometries were optimized at the same DFT level. Eventually the energies of **2a**, **TS**, and **3a** were refined at the PCM(toluene)/B3LYP-D3/6-311+G(d,p) level.[18]

With achiral ligands **L5a-c**, pathways leading to carbolithiation products (*R*)-**3a** and (*S*)-**3a** are isoenergetic. As a consequence, our calculations were restricted to a sole configuration of the newly formed indan ring, arbitrarily chosen as the *S* configuration. Our investigation primarily focused on the two symmetric additives TMEDA (**L5a**) and DME (**L5b**). As the five-membered chelate ring formed between the lithium atom and the ligand adopts either a λ or δ half-chair conformation,[19] two favored diastereomeric TSs, both leading to the S_{C2}-indan, were identified for each ligand (Figure 2).

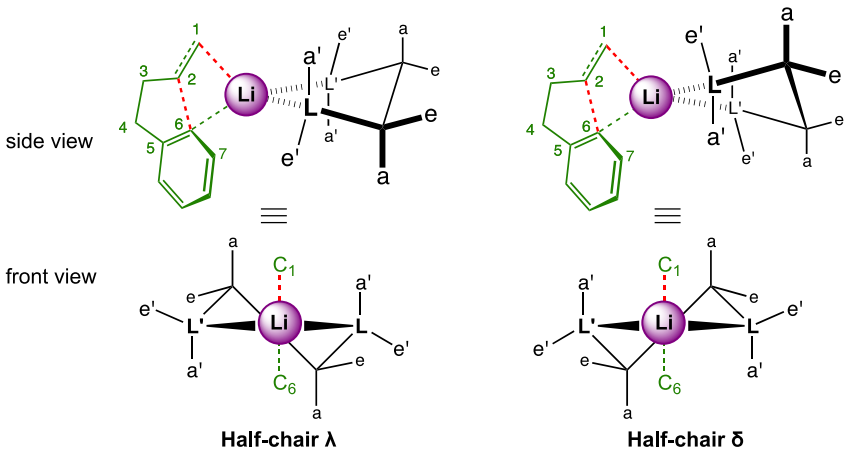

Figure 2. Representations of diastereomeric carbolithiation TSs stemming from λ and δ half-chairs of the lithium-ligand chelate ring.

Figure 3 shows, for **L5a** (top) and **L5b** (bottom), the Gibbs free energy profiles of the cyclization **2a** → TS → **3a** (left part), the geometries of the diastereomeric TS (central part) and their electronic (ΔΔE), enthalpic ($\Delta\Delta H_{298}$) and Gibbs free ($\Delta\Delta G_{298}$) energy differences (right part).[20]

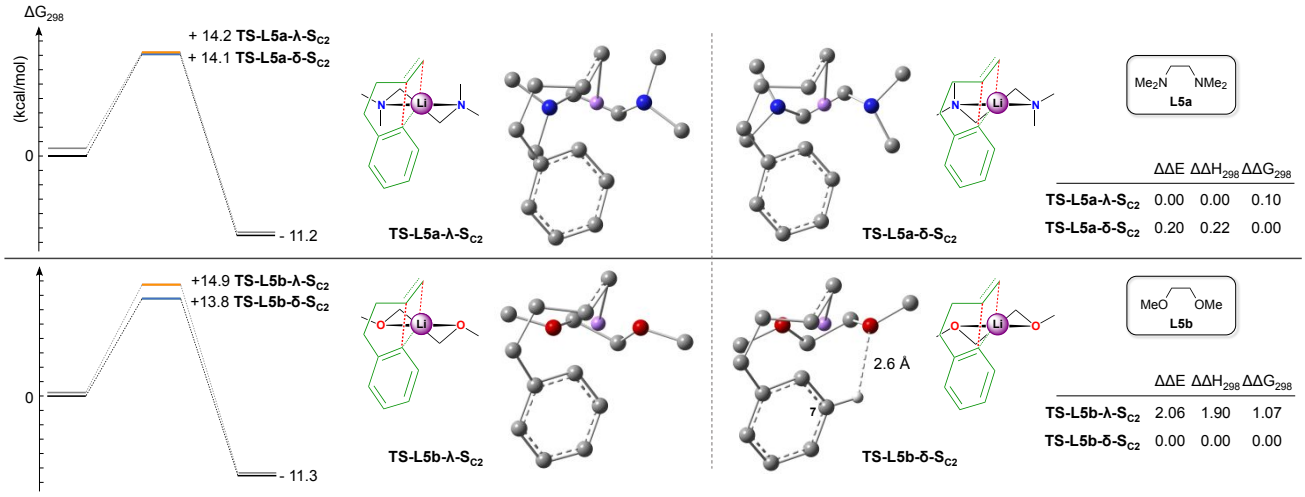

Figure 3. Computation of achiral ligands **L5a**- and **L5b**-mediated cyclization of **2a** (most H atoms are omitted).

The Gibbs free energies of activation $\Delta G_{298}^{\ddagger}$ (**2a** → TS) are around 14 kcal/mol for both ligands and final complexes **3a** are more stable than the starting complexes **2a** by 11 kcal/mol. These values are consistent with an irreversible cyclization at room temperature. Noteworthy, the two most favored **L5b**-mediated TSs exhibit both methyl groups on the ether functions in pseudo-equatorial (e') positions. Their analogs with one methyl group in a pseudo-axial (a') position were found to be at least 2 kcal/mol ($\Delta\Delta G_{298}$) above **TS-L5b-δ-S_{C2}** and are thus neglected to focus the following discussion on a reasonable number of favored TSs.

While the TMEDA diastereoisomeric transition states, **TS-L5a-λ-S_{C2}** and **TS-L5a-δ-S_{C2}**, are energetically similar, in the case of DME **TS-L5b-δ-S_{C2}** is favored over **TS-L5b-λ-S_{C2}** by more than 1 kcal/mol. This difference could originate from the pseudo-axial position of one oxygen's lone pair in **TS-L5b-δ-S_{C2}** which points toward an aromatic hydrogen (H-C^7) with a distance of 2.6 Å, consistent with a weak hydrogen bond length.[21] To further support this hypothesis, a topological analysis of the electron density, based on Bader's theory of atoms in molecules (QTAIM) was conducted.[10, 22] A bond critical point (BCP) is indeed found between one oxygen atom and H-C^7 with an electron density (ρ = 0,0084 au) and its Laplacian value ($\nabla^2\rho$ = 0,029 au) consistent with a weak hydrogen bond.[23, 21c]

Switching to amino ether **L5c** introduces additional complexity since this hybrid ligand forms unsymmetrical half-chair chelates. As a result the lithium atom becomes stereogenic and accordingly four TSs were computed: two half-chair conformations with an *S* configuration of the lithium atom (S_{Li}) and two with the opposite *R* configuration (R_{Li}) (Figure 4).[24]

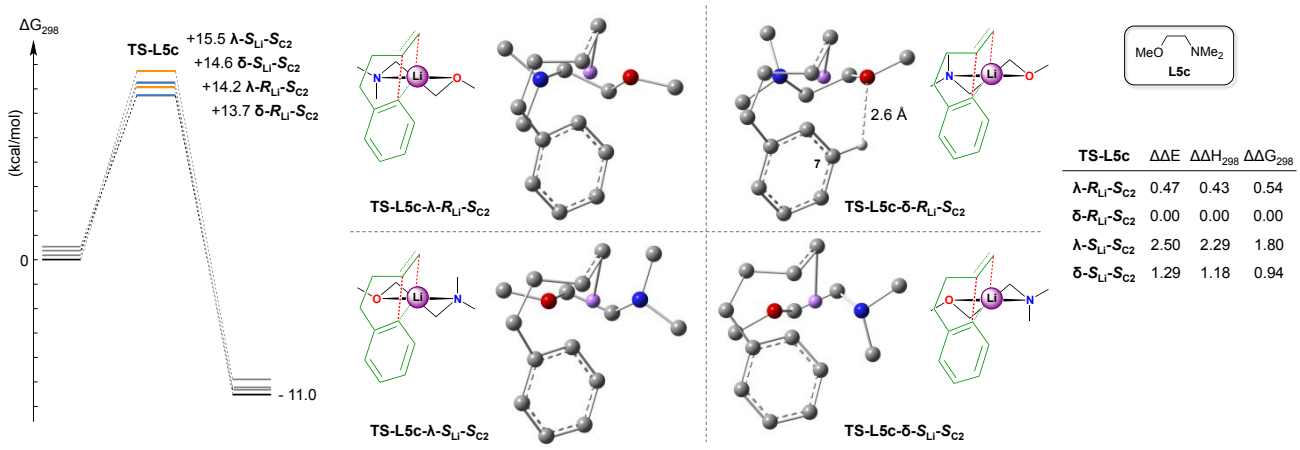

TS-L5c	ΔΔE	ΔΔH298	ΔΔG298
λ-R_{Li}-S_{C2}	0.47	0.43	0.54
δ-R_{Li}-S_{C2}	0.00	0.00	0.00
λ-S_{Li}-S_{C2}	2.50	2.29	1.80
δ-S_{Li}-S_{C2}	1.29	1.18	0.94

Figure 4. Computation of achiral ligand **L5c**-mediated cyclization of **2a** (most H atoms are omitted).

These four TSs show a pseudo-equatorial methyl group on the ether function and **L5c**-mediated TSs presenting a pseudo-axial methyl group were found to be significantly unfavored.[25] Furthermore, as observed with DME, the most favored TS, **TS-L5c-δ-R_{Li}-S_{C2}**, presents an oxygen lone pair likely bonding with the aromatic H-C^7 (2,6 Å), confirmed by the QTAIM analysis results (ρ = 0,0088 au; $\nabla^2\rho$ = 0,030 au). This supports the hypothesis that the energy difference between the diastereomeric TSs might be driven by favorable weak interactions (vide infra).

Chiral (pseudo) C_2-symmetric 1,2-bidentate ligands

We then modeled the transition structures for the cyclohexyl-based ligands **L4a-c** (Figure 1). The six-membered ring of the carbon skeleton is locked in the chair conformation in which both dimethylamino and/or methoxy groups are equatorial. As a result, the fused five-membered chelate formed between (*S,S)*-**L4** ligands and the lithium atom is frozen in the δ half-chair conformation. Figure 5 shows the two diastereomeric transition states leading to either *R*-indan (R_{C2}) or *S*-indan (S_{C2}) for diamino and diether ligands **L4a** and **L4b** as well as the related energy profiles.

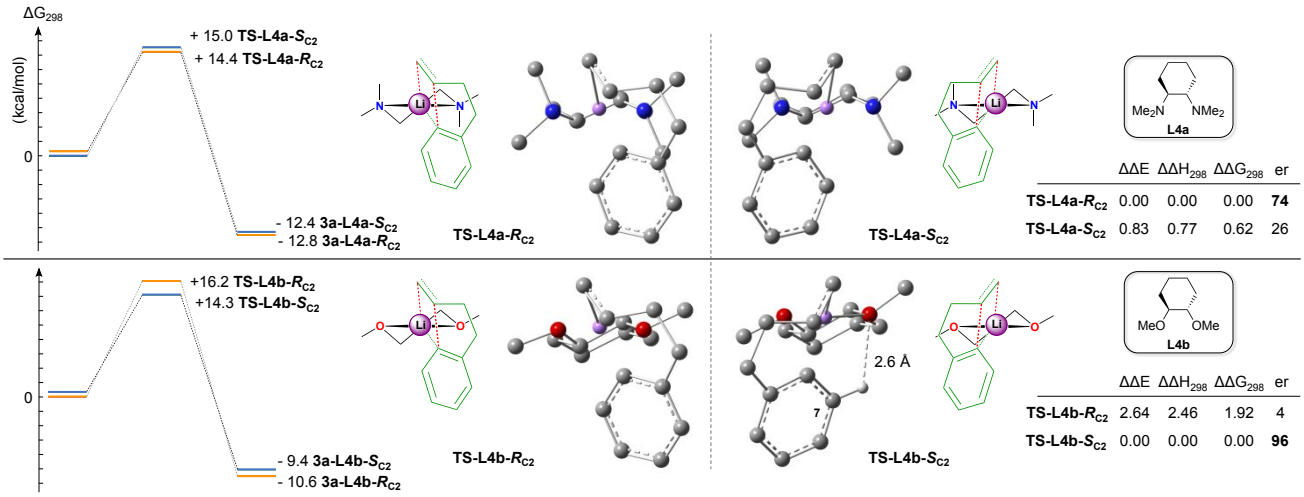

Figure 5. Computation of chiral ligand **L4a-b**-mediated cyclization of **2a** (most H atoms are omitted).

As with achiral ligands **L5**, these free energy profiles are consistent with irreversible carbolithiation reactions. Moreover, the energy profile with diether **L4b** shows **3a-L4b-R_{C2}** and **3a-L4b-S_{C2}** to be respectively the thermodynamic and the kinetic products of this process. As the experimental major enantiomer of the indan is S_{C2}, this is an additional proof of the kinetic control of this process.

According to the Curtin-Hammett principle,[26] the enantioselectivity of the carbolithiation should be in correlation with the difference between the Gibbs free energies of the two competing diastereoisomeric TSs ($\Delta\Delta G_{298}$). In the case of diamine (*S*,*S*)-**L4a**, the difference between **TS-L4a-R_{C2}** and **TS-L4a-S_{C2}** is 0.62 kcal/mol in favor of the formation of the (*R*)-indan. According to Boltzmann distribution law, at 298K, this gap should lead to a *R*:*S* ratio of 74:26. This theoretical result is, indeed, in good agreement with the experimental 71:29 e.r. observed when the carbolithiation is conducted with (*S*,*S*)-**L4a** at room temperature. The slightly lower experimental stereoselectivity could arise from minor background (unliganded) reaction or secondary reaction pathways involving for example oligomeric organolithium structures, which have not been accounted for in the present study. In the case of diether (*S*,*S*)-**L4b**, the difference between the two diastereomeric TSs is completely reversed in favor of the (*S*)-indan in a predicted 4:96 (*R*:*S*) ratio. As discussed previously with achiral **L5b** (Figure 3), the stabilization of **TS-L4b-S_{C2}** is likely based on a weak stabilizing hydrogen bond between an oxygen atom and the aromatic hydrogen H-C^7 (2,6 Å; ρ = 0,0091 au; $\nabla^2\rho$ = 0,031 au). Again, the experimental stereoselectivity obtained with **L4b** (9:91 *R*:*S*) is rather consistent with the predicted enantiomeric ratio, which confirms the relevance of our model.

Eventually, a similar analysis was conducted to compute (*S*,*S*)-**L4c** transition states. Like achiral **L5c** (vide supra), this unsymmetrical ligand generates two configurations of the lithium atom (R_{Li} and S_{Li}). Accordingly, four diastereomeric TSs have been modeled (Figure 6).

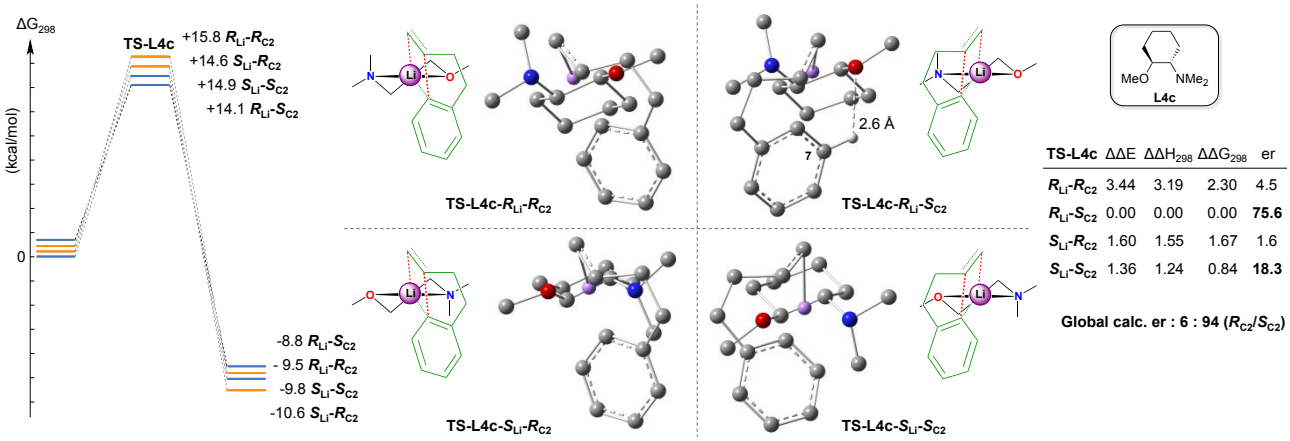

Figure 6. Computation of chiral ligand **L4c**-mediated cyclization of **2a** (most H atoms are omitted).

As discussed above, **TS-L4c-*R*$_{Li}$-*S*$_{C2}$** is presumably stabilized by the existence an C^7-H•••O weak bond (2.6 Å; electron density ρ = 0,008 au; Laplacian value $\Delta^2\rho$ = 0,028 au). This TS is indeed enthalpically favored by more than 1 kcal/mol over the three others diastereomeric TS. Although $\Delta\Delta G_{298}$ values follow the same trend as $\Delta\Delta H_{298}$ (enthalpic control of stereoselectivity), the influence of the entropy factor is not negligible in the case of amino ether **L4c**. **TS-L4c-*R*$_{Li}$-*R*$_{C2}$** and **TS-L4c-*S*$_{Li}$-*S*$_{C2}$**, which are respectively 3.19 and 1.24 kcal/mol over the most favored **TS-L4c-*R*$_{Li}$-*S*$_{C2}$** in terms of enthalpy energy ($\Delta\Delta H_{298}$), see their Gibbs free energy difference ($\Delta\Delta G_{298}$) with the latter reduced to 2.30 and 0.84 kcal/mol. In other words, the entropic terms ($-T\Delta\Delta S$) relative to **TS-L4c-*R*$_{Li}$-*S*$_{C2}$**, are -0.89 kcal/mol for **TS-L4c-*R*$_{Li}$-*R*$_{C2}$** and -0.40 kcal/mol for **TS-L4c-*S*$_{Li}$-*S*$_{C2}$**. It can be inferred that the entropy factor is probably more detrimental to the TSs featuring the alkenyl chain of the substrate close to the dimethylamino side of the ligand. This results in noticeable contributions of these two TSs to the predicted stereoselectivity of (*S*,*S*)-**L4c**-mediated reaction, which reaches an enantiomeric ratio of 6:94 (*R*:*S*). This theoretical value is slightly lower than the one calculated for the diether ligand (*S*,*S*)-**L4b** and this trend is reflected in the experimental stereoselectivity levels of 15:85 e.r. with (*S*,*S*)-**L4c** against 9:91 e.r. with (*S*,*S*)-**L4b**.

It should be noted that although the activating energies of the carbolithiation $\Delta G^{\ddagger}_{298}$ are similar for the diamine, diether and amino ethers ligands, it does not necessarily reflect the rate of the global process. In fact, these values are not in accordance with our experimental observation that indan **4a** and indoline **4b** are formed more rapidly when ligands featuring amine functions are used. [27] This suggests that the rate-determining step of this

transformation would not be the stereo-determining cyclization step but more likely the formation of the monomeric lithium-olefin complex **2a** from aggregated form(s) of the aryllithium and ligand complex (Scheme 2).[8b]

Distortion / Interaction analysis

To complete our understanding of the stereo-determining factors of this reaction, a distortion/interaction (D/I) analysis was conducted. This consists in investigating the activation barrier ($\Delta E^{\ddagger}$) of a reaction as a combination of a distortion energy and an interaction energy (Equation 1).[28] The distortion energy (or activation strain), ΔE_{dist}, is the energy required by the reactants to reach their transition-state geometries as individual components whereas the interaction energy, ΔE_{int}, represents the balancing favorable bonding between these components in the TS. In the present case, we fragmented precomplex **2a** and the TS into the ligand on one hand and the aryllithium on the other (Figure 7). For each TS and corresponding precomplex **2a**, the distortion energy could be then decomposed into 1) the ligand-aryllithium dissociation energy in precomplex **2a**, $\Delta E_{dist\text{-}\mathbf{2a}}$, 2) the distortion energy of the substrate, $\Delta E_{dist\text{-}sub}$, 3) the distortion energy of the ligand, $\Delta E_{dist\text{-}lig}$ (Equation 2).

$$\Delta E^{\ddagger} = \Delta E_{dist} + \Delta E_{int} \qquad (1)$$

$$\Delta E_{dist} = \Delta E_{dist\text{-}\mathbf{2a}} + \Delta E_{dist\text{-}sub} + \Delta E_{dist\text{-}lig} \qquad (2)$$

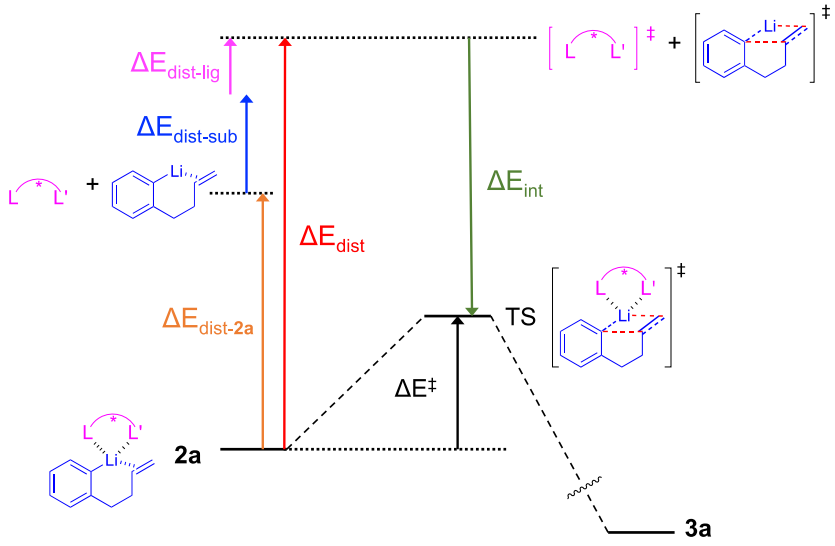

Figure 7. Distortion/Interaction analysis: decomposition of activation barrier into a distortion energy ($\Delta E_{dist\text{-}\mathbf{2a}}$+$\Delta E_{dist\text{-}sub}$+$\Delta E_{dist\text{-}lig}$) and an interaction energy ΔE_{int}.

The results of the D/I analysis are presented using the most stable precomplex **2a** as the energy reference point for each ligand (Figure 8).

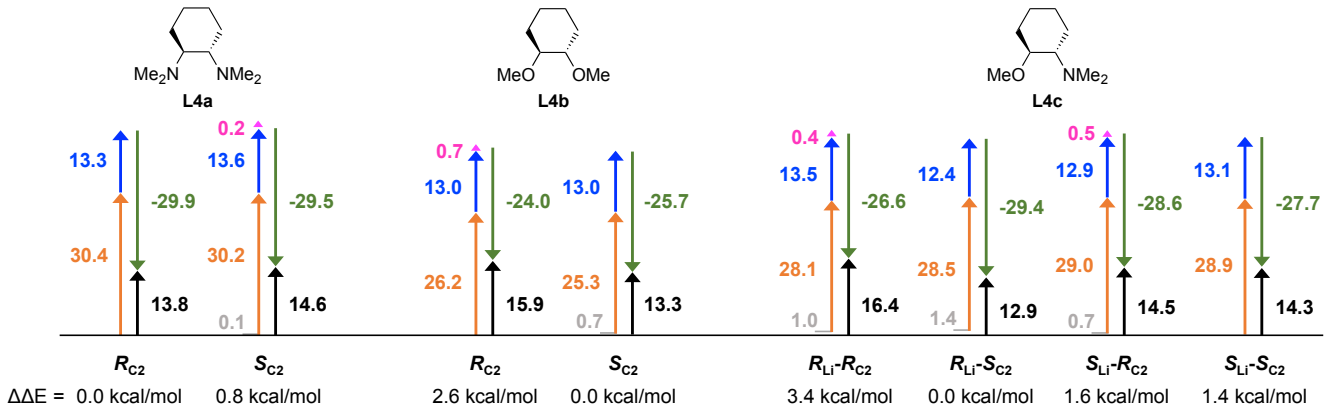

Figure 8. D/I analysis results for all TSs of **L4a-c**-mediated carbolithiation ($\Delta E_{dist\text{-}\mathbf{2a}}+\Delta E_{dist\text{-}sub}+\Delta E_{dist\text{-}lig}$ and ΔE_{int} in kcal/mol)

The relative energy of the less stable precomplexes **2a** is indicated by the value in grey. Regardless of the ligand, the energy profiles show substrate distortion energies $\Delta E_{dist\text{-}sub}$ about 13 kcal/mol while ligand distortion energies $\Delta E_{dist\text{-}lig}$ are systematically lower than 1 kcal/mol. Furthermore, the strength of the ligand-organolithium bonding, in both the precomplex **2a** ($\Delta E_{dist\text{-}\mathbf{2a}}$) and the TS ($\Delta E_{int}$), decreases in the following order diamine **L4a** > amino ether **L4c** > diether **L4b**. This agrees with the relative Lewis base strength of the amine and ether functions. More importantly, the distortion / interaction study allows to understand which energy factor drives the stereoselectivity of the reaction in terms of difference of activation barriers ($\Delta\Delta E^{\ddagger}$) between the diastereoisomeric TSs of each ligand. For diamine **L4a**, the small energy difference $\Delta\Delta E^{\ddagger}$ between the R_{C2} and S_{C2} pathways (0.8 kcal/mol) results from small contributions of unfavorable $\Delta E_{dist\text{-}sub}$ and $\Delta E_{dist\text{-}lig}$ in the S_{C2} pathway as well as a slightly more favorable ΔE_{int} in the R_{C2} pathway. By contrast, for diether **L4b**, the more important $\Delta\Delta E^{\ddagger}$ (2.6 kcal/mol), in favor of the S_{C2} pathway, mainly arises from significant favorable ligand-aryllithium interactions in the TS (ΔE_{int} = 25.7 kcal/mol for S_{C2} and ΔE_{int} = 24.0 kcal/mol for R_{C2}). To a lesser extent the same statement can be made in the case of amino ether **L4c**, for the R_{Li}-S_{C2} pathway presents the greater favorable ΔE_{int}. Actually, both the S_{C2} pathway with **L4b** and the R_{Li}-S_{C2} pathway with **L4c**, for which the AIM analysis reveal favorable weak hydrogen bond in the corresponding TSs, are the only energy profiles to present stronger stabilizing interactions between the ligand and the organolithium in the TS (ΔE_{int}) than in the precomplex **2a** ($\Delta E_{dist\text{-}\mathbf{2a}}$). However, the R_{Li}-S_{C2} pathway with **L4c** appears to be also favored by lowest distortion energies: 12.4 kcal/mol for $\Delta E_{dist\text{-}sub}$ and virtually non-existent $\Delta E_{dist\text{-}lig}$.

Non-covalent interactions analysis

To further identify the presence of non-covalent interactions in these TSs, a non-covalent interactions (NCI) analysis was conducted.[29] This analysis allows the visualization of the reduced density gradient isosurfaces, for which the color code is green for weakly attractive, blue for strongly attractive and red for strongly repulsive interactions. Figure 9 shows the interactions taking place in diastereomeric TSs with **L4a** and **L4b**.

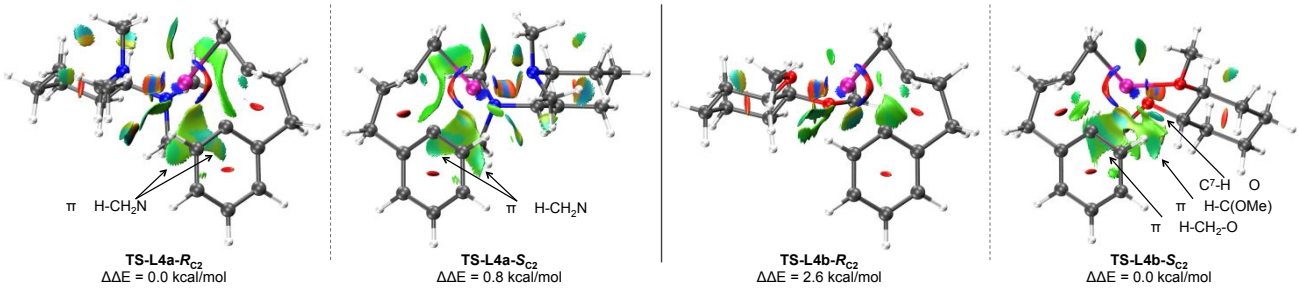

Figure 9. Non-covalent interactions analysis: Visualization of the reduced density gradient isosurfaces for **L4a-b** TSs (density cutoff of 0.4 au).

Diastereomeric transition states with diamine **L4a**, **TS-L4a-R_{C2}** and **TS-L4a-S_{C2}**, exhibit comparable weak favorable interactions, including weak hydrogen bonds between the electron-rich π system and hydrogens from one of the NMe group (π•••H-CH_2N).[30] This is consistent with their limited electronic energy difference (ΔΔE = 0.8 kcal/mol). By contrast, **TS-L4b-S_{C2}** clearly presents a more prominent number of stabilizing interactions than **TS-L4b-R_{C2}**. At least three weak hydrogen bond types, C^7-H•••O, π•••H-CH_2O and π•••H-C(OMe) appear in **TS-L4b-S_{C2}**. This suggests that the significant electronic energy gap between these two diastereomeric TSs (ΔΔE = 2.6 kcal/mol) arises from a sum of multiple weakly attractive interactions between the ligand and the substrate. For amino ether **L4c** TSs, the NCI analysis also supports the presence of numerous noncovalent interactions operating in concert in the most stable **TS-L4c-R_{Li}-S_{C2}** (Figure 10).

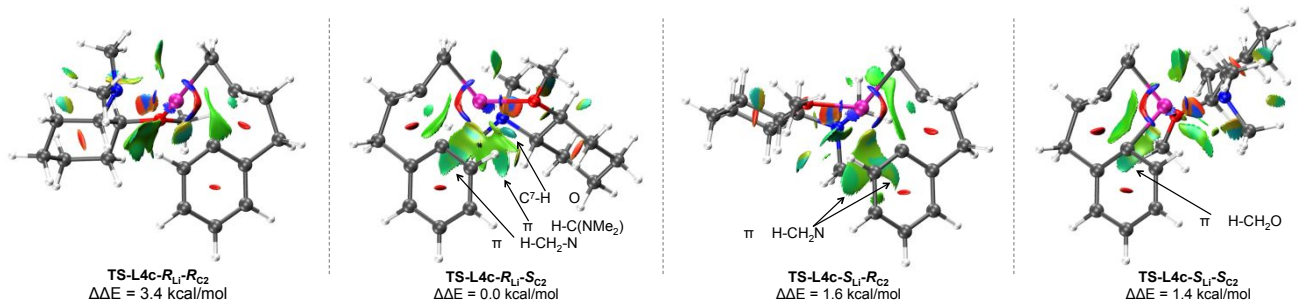

Figure 10. Non-covalent interactions analysis: Visualization of the reduced density gradient isosurfaces for **L4c** TSs (density cutoff of 0.4 au).

Favorable interactions between the π system and the ligand, π•••H-CH_2N and π•••H-CH_2O, can also be noticed in **TS-L4c-S_{Li}-R_{C2}** and **TS-L4c-S_{Li}-S_{C2}** respectively whereas in **TS-L4c-R_{Li}-R_{C2}** no NMe or OMe group is facing the aromatic ring and therefore no significant π•••H bond is observed. This is in good agreement with the relative electronic energies of these three less favorable TSs (Figure 6).

Achiral *versus* chiral 1,2-bidentate ligands modeling

When considered as *isolated* entities, the λ and δ half-chair chelates formed from lithium and achiral ligand **L5** are enantiomers. Accordingly, the λ half-chair TS leading to the (S_{C2})-indan (**TS-L5-λ-S_{C2}**) is enantiomeric and so energetically equal to the δ half-chair TS leading to the (R_{C2})-indan (**TS-L5-δ-R_{C2}**).[31] As a consequence, it can be foreseen from the energy difference values depicted in figures 3 and 4, how a given half-chair would favor the formation of one indan enantiomer. Table 1 presents the ratios of R_{C2} / S_{C2} indan formation 1) for the δ half chair of achiral ligands **L5** (calculated value) 2) for chiral ligands **L4** of (*S*,*S*) absolute configuration (experimental and calculated values).

Table 1. Comparison of (virtual) enantioselectivities for a given half-chair with achiral ligands **L5** and for a given configuration of chiral ligands **L4**.

	δ(R_{C2}) / δ(S_{C2}) TSs ratio for achiral ligands **L5**			R_{C2} /S_{C2} TSs ratio for (*S*,*S*)-**L4** ligands		
	L5a	**L5b**	**L5c**	**L4a**	**L4b**	**L4c**
Experimental	-	-	-	71:29	9:91	15:85
Calc. from $\Delta\Delta G_{298}$	46:54	14:86	27:73	74:26	4:96	6:94

These ratios were calculated using Boltzmann distribution law, at 298K, from the Gibbs free energy difference $\Delta\Delta G_{298}$ between the diastereomeric TSs. For the ethereal achiral ligands **L5b-c**, the δ half-chair TSs give predominantly the (S_{C2})-indan. In contrast, for the diamino ligand **L5a**, the δ half-chair TSs lead to almost equimolar amount of (S_{C2})- and (R_{C2})-indans. The experimental and theoretical results with (*S*,*S*)-**L4a-c**, which locks the lithium chelate as a δ half-chair, follow similar trends : the relative efficiency is also diether > amino ether > diamine and, for the ethereal ligands, the sense of stereoinduction is effectively in favor of the formation of S_{C2}-indan. It appears

that to reach high enantioselectivity with a chiral 1,2-bidentate ligand, its achiral parent must present a noticeable discrimination between the diastereomeric pathways stemming from the formation of the two half-chairs of its lithium chelate. Therefore, the preliminary computational study on 1,2-bidentate achiral ligands already allows 1) to identify the most promising chelating patterns between different classes of ligands, 2) to predict the sense of stereoinduction for the related chiral ligand, by considering the preferred half-chair conformation of its lithium chelate - this preferential conformation is governed by the absolute configuration of the ligand.

From a more general point of view, what could this mean for the modeling of asymmetric reactions mediated by 1,2-bidentate ligands? This implies that computing only one stereoselective course of a reaction with different achiral 1,2-bidentate ligands for both their λ or δ half-chair conformations, should allow to relatively predict how parent chiral 1,2-bidentate ligands will perform as chiral inducers, provided that their absolute configurations clearly favor one of these chelate conformations. Therefore, the screening of chelating patterns for the design of new 1,2-bidentate chiral ligands could be expedited thanks to reasonable calculation times reduced by neglecting the carbon backbone of such chiral ligands.

Conclusions

In summary we have conducted the first experimental and theoretical formal comparison of three 1,2-bidentate ligand classes with the intramolecular carbolithiation as a model reaction. For (pseudo) C_2-symmetric cyclohexanediamine, -diether and -amino ether ligands, modeling of the diastereomeric transition states led to conclusive theoretical levels of stereoselectivity matching the experimental results. The distortion/interaction analysis suggest that the high levels of stereoinduction with the ethereal ligands originate from stabilizing interactions in their most favorable transition states. AIM and NCI indeed allowed for the identification of several weak hydrogen bonds between the substrate and the ligands in the TS. These interactions appear as largely responsible for the discrimination between the diastereomeric reaction pathways in the case of the diether and amino ether ligands. Interestingly, modeling the reaction with related *achiral* 1,2-bidentate ligands already leads to the identification of diastereomeric TSs due to the formation of λ and δ half-chair conformations of the lithium chelate. Comparing the relative energy differences of these TSs allows for the qualitative prediction of the sense of stereoinduction and the relative efficiency of the (pseudo) C_2-symmetric chiral ligands. This paves the way for

simplified theoretical studies of chiral 1,2-bidentate ligands-mediated asymmetric additions. Ongoing experimental and computational investigations on C_1-symmetric ligands-mediated carbolithiation will be reported in due course.

Experimental section

General information

All air- and moisture-sensitive manipulations were performed under argon atmosphere with anhydrous solvents in flame-dried glassware. The solvents (THF, CH_2Cl_2, Et_2O, Toluene) were dried by activated alumina column (glass technology GTS 100). *t*-BuLi was purchased as 1.7 M solution in pentane and was titrated periodically against *N*-benzylbenzamide.[32] Other commercially available reagents were used without further purification, unless otherwise indicated. Flash column chromatography was carried out using Merk Kieselgel 60 silica gel (particle size : 32-63 Å). Analytical TLC was performed using Merk precoated silica gel 60 F-254 sheets with spot detection under UV light or using potassium permanganate stain or cerium ammonium molybdate stain. ^{1}H and ^{13}C {^{1}H} NMR spectra were recorded on a BRUKER DPX 200 or on a BRUKER Advance 400 spectrometer. Coupling constants *J* are reported in Hertz (Hz). Multiplicity is indicated as follow, s (singlet), d (doublet), t (triplet), q (quartet), sext (sextuplet), sept (septuplet), oct (octuplet), dd (doublet of doublet), bs (broad singlet), m (multiplet) and “app.” stands for apparent. IR spectra were recorded neat or as thin films using a Nicolet Avatar 370 DTGS FT-IR spectrometer. Melting points were measured on a Melting Point B-540 apparatus and are uncorrected. Optical rotations were measured on Jasco P-2000 polarimeter using a quartz cell (l=10 cm), with a high-pressure sodium lamp (λ = 589 cm). $[\alpha]_D$ values are given in 10^{-1}deg.cm^2.g^{-1}. High Resolution Mass Spectrometry (HRMS) was performed on a Waters Micromass GTC Premier spectrometer or Bruker MicroTOF QIII spectrometer. 2-bromo-1-(3-butenyl)benzene[33] (**1a**) was synthesized by the reaction of 2-bromobenzyl bromide[34] and allylmagnesium bromide and *N*,*N*-diallyl-2-bromoaniline[6d] (**1b**) by *N*,*N*-diallylation of 2-bromoaniline.

Ligands synthesis

(1S,2S)-N¹,N¹,N²,N²-tetramethylcyclohexane-1,2-diamine (**L4a**). Ligand **L4a** was synthesized via resolution of racemic *trans*-1,2-cyclohexanediamine using D-(-)-tartaric acid followed by Eschweiler-Clarke reaction on the tartrate salt. [3c, 35]

(1S,2S)-1,2-dimethoxycyclohexane (**L4b**). (*1S, 2S*)-cyclohexane-1,2-diol[36] (2.64 g, 22.7 mmol) was added portionwise to a suspension of sodium hydride (3.27 g, 136.2 mmol, 6 equiv) in anhydrous Et_2O (100 mL). The mixture was stirred at room temperature for 4h. After cooling at 0°C, methyl iodide (14 mL, 227 mmol, 10 equiv) was added dropwise. After 24h stirring at reflux (heating mantle), water (5 mL) was added dropwise and the mixture was vigorously stirred for 1h at room temperature. The reaction mixture was extracted with Et_2O (3 ×50 mL) and the combined organic layers were dried over $MgSO_4$. Distillation on CaH_2 at reduced pressure afforded (*S*,*S*)-1,2-dimethoxycyclohexane (**L4b**) (2.78 g, 85 %) as a colorless oil. Bp = 29 °C at 0.2 mbar. $[\alpha]_D^{24}$: + 53.6 (c = 1.05, $CHCl_3$). ^{1}H NMR (400 MHz, $CDCl_3$) δ: 3.42 (s, 6H, $2OCH_3$), 3.09 - 3.07 (m, 2H, 2CH), 2.05- 2.01 (m, 2H, CH_2), 1.68 - 1.64 (m, 2H, CH_2), 1.25 - 1.18 (m, 4H, $2CH_2$). ^{13}C {^{1}H} NMR (100 MHz, $CDCl_3$) δ: 82.5 (2CH), 57.2 ($2CH_3$), 29.3 ($2CH_2$), 23.6 ($2CH_2$). HRMS (Cl^+) m/z: $[M+H]^+$: Calcd for $C_8H_{17}O_2$ 145.1229; Found 145.1222.

(1S,2S)-2-methoxy-N,N-dimethylcyclohexanamine (**L4c**). *Step A* : di-*tert*-butyl dicarbonate (8.12 g, 37.2 mmol, 1.2 equiv) was added slowly to a solution of (1*S*,2*S*)-2-(methylamino)cyclohexanol[37] (4.0 g, 31 mmol, 1 equiv) in 2M $NaOH_{(aq)}$ (81 mL). The mixture was stirred overnight at 30 °C (heating mantle) prior to the addition of CH_2Cl_2 (40 mL). The layers were separated and the aqueous layer was extracted with CH_2Cl_2 (3×40 mL). The combined organic phases were dried over Na_2SO_4, filtered and concentrated under vacuum providing crude *tert*-butyl (1*S*,2*S*)-2-hydroxycyclohexyl(methyl)carbamate (5.75 g, 81 %). *Step B* : Methyl iodide (2.6 mL, 42,2 mmol, 1.7 equiv) and NaH (60% in mineral oil, 1.7 g, 42.2 mmol, 1.7 equiv) were successively added to a solution of crude *tert*-butyl (1*S*,2*S*)-2-hydroxycyclohexyl(methyl)carbamate (5,7g, 24.8 mmol, 1 equiv) in THF (70 mL) at 0 °C. The reaction mixture was stirred overnight at room temperature prior to the careful addition of saturated NH_4Cl(aq) (50 mL) at 0 °C. The aqueous phase was extracted with EtOAc (3×50 mL). The combined organic layers were dried over Na_2SO_4, filtered and concentrated under vacuum. Chromatography on silica gel (cyclohexane / EtOAc: 80/20 → 70/30) gave *tert*-butyl (1*S*,2*S*)-2-methoxycyclohexyl(methyl)carbamate (4.63 g, 77 %) as a colorless oil. $[\alpha]_D^{20}$: +11.9 (c = 1.15, $CHCl_3$). ^{1}H NMR (400 MHz, DMSO) δ: 3.61 (bs, 1H, CH), 3.22-3.12 (m, 4H, OCH_3+CH), 2.68 (s, 3H, NCH_3), 2.11 (m, 1H, CH_2), 1.68-1.63 (m, 2H, CH_2), 1.58-1.43 (m, 2H, $2CH_2$), 1.39 (s, 9H, $C(CH_3)_3$), 1.22-1.01 (m, 3H, $2CH_2$). ^{13}C {^{1}H} NMR (100

MHz, DMSO) δ: 155.0 (C=O), 78.1 (CH), 77.8 (C), 59.0 (CH), 55.0 (OCH_3), 30.2 (NMe), 29.0 ($2CH_2$), 28.1 ($3CH_3$), 24.8 (CH_2), 23.8 (CH_2). IR (neat) ν : 2931, 1687, 1365, 1149, 1100, 944 cm^{-1}. HRMS (ESI^+) m/z: $[M+H]^+$ Calcd for $C_{13}H_{25}NO_3Na$ 266.1727; Found 266.1726. TLC : R_f 0.43 (cyclohexane / EtOAc : 6 /2, $KMnO_4$). *Step C* : To a suspension of $LiAlH_4$ (2.2 g, 57 mmol, 3 equiv) in dry Et_2O (35 mL) at 0 °C was added a solution of crude *tert*-butyl (1*S*,2*S*)-2-methoxycyclohexyl(methyl)carbamate (4,43g, 19,0 mmol, 1 equiv) in dry Et_2O (70 mL). The reaction mixture was refluxed overnight (heating mantle), cooled to 0 °C and diluted with Et_2O (25 mL). After the careful portionwise addition of $Na_2SO_4.10H_2O$ (3 equiv), the resulting mixture was stirred at room temperature for 1 h. The solids were removed by filtration through a pad of celite and were washed with Et_2O (25 mL). The filtrate was dried over Na_2SO_4 and diethyl ether was removed by simple distillation. Bulb-to-bulb distillation (150 °C, 300 mbar) gave (1*S*,2*S*)-2-methoxy-*N*,*N*-dimethylcyclohexanamine (**L4c**) (2.43 g, 81 %) as a colorless oil. $[\alpha]_D^{20}$: + 55.8 (c = 1.0, $CHCl_3$). ^1H NMR (400 MHz, $CDCl_3$) δ: 3.31 (s, 3H, OCH_3), 3.05 (m, 1H, CH), 2.32 (m, 1H, CH), 2.26 (s, 6H, $N(CH_3)_2$), 2.11 (m, 1H, CH_2), 1.74 (m, 1H, CH_2), 1.66-1.64 (m, 2H, CH_2), 1.14-1.07 (m, 4H, $2CH_2$). ^{13}C {^1H} NMR (100 MHz, $CDCl_3$) δ: 79.9 (CH), 66.9 (CH), 55.9 (OCH_3), 41.0 ($N(CH_3)_2$), 30.3 (CH_2), 25.0 (CH_2), 24.4 (CH_2), 23.8 (CH_2). IR (neat) ν : 2928, 2859, 2820, 2775, 1452, 1102 cm^{-1} HRMS (ESI^+) m/z: $[M+H]^+$ Calcd for $C_9H_{20}NO$ 158.1539; Found 158.1548.

Carbolithiation reactions – General procedure for the preparation of indane 4a and indoline 4b

A solution of ligand (2.2 equiv) in anhydrous toluene (4 mL) was cooled to –78 °C in a flame-dried Schlenk tube under argon. *t*-BuLi in pentane (2.2 equiv) was added dropwise and an intense yellow solution formed. A solution of bromoarene **1** (0.5 mmol, 1 equiv) in anhydrous toluene (1 mL) was then added dropwise and the mixture was stirred for an additional 10 min at –78 °C. The reaction vessel was then transferred to a constant-temperature bath maintained at the specified temperature (20 °C for **1a**, –40 °C for **1b**) and stirred for 1–3 h. The reaction mixture was then recooled to –78 °C, quenched by the addition of 1 mL of deoxygenated dry MeOH, and allowed to reach room temperature. An aqueous saturated NH_4Cl solution (5 mL) was added, the phases were separated, and the organic layer was dried over $MgSO_4$. The enantiomeric ratios were determined by CSP-GC analysis of an aliquot of the organic layer.

(S)-1-methylindan **(4a).** Following the carbolithiation general procedure, the ligand (1.1 mmol), *t*-BuLi (0.72 mL, 1.53 M in pentane, 1.1 mmol) and 2-bromo-1-(3-butenyl)benzene (**1a**) (106 mg, 0.5 mmol) were reacted at rt for 1 h.

After standard work-up, the enantiomeric ratio of **4a** was determined by chiral stationary-phase gas chromatography (CSP-GC) (30 m × 250 μm × 0.25 μm Rt-βDEXcst column; Carrier gas : helium ; 1.5 mL/min ; Injector : set at 220 °C ; Detector : FID set at 230 °C, Oven temp. : 90 °C (hold 5 min.) to 140 °C at 5 °C/min): (*R*)-**4a** tr = 11.4 min, (*S*)-**4a** tr = 11.6 min. An analytically pure sample of **4a** was obtained by flash chromatography on silica gel (pentane). Colorless oil. For an enantiomeric ratio of 9:91 (*R*/*S*), $[\alpha]_D^{24}$ –2.7 (*c* = 1.1, $CHCl_3$) (lit. [38] er = 94:6 (*R*/*S*) : $[\alpha]_D^{24}$ +2.35 (*c* = 1.0, $CHCl_3$)). ^{1}H NMR (400 MHz, $CDCl_3$) δ: 7.30–7.10 (m, 4H), 3.18 (m, 1H), 2.95–2.68 (m, 2H), 2.30 (m, 1H), 1.60 (m, 1H), 1.29 (d, *J* = 6.9 Hz, 3H). ^{13}C {^{1}H} NMR (100 MHz, $CDCl_3$) δ: 148.8, 143.9, 128.5, 126.1, 124.3, 123.2, 39.4, 34.8, 31.5, 19.9 (consistent with lit.[6a]).

(R)-1-allyl-3-methylindoline (**4b**). Following the carbolithiation general procedure, the ligand (1.1 mmol), *t*-BuLi (0.72 mL, 1.52 M in pentane, 1.1 mmol) and *N*,*N*-diallyl-2-bromoaniline (**1b**) (126 mg, 0.5 mmol) were reacted at –40 °C for 3 h. After standard work-up, the enantiomeric ratio of **4b** was determined by chiral stationary-phase gas chromatography (CSP-GC) (30 m × 250 μm × 0.25 μm CP-Chirasil-Dex CB column; carrier gas : helium ; 1.5 mL/min ; Injector : set at 220 °C ; Detector : FID set at 230 °C, Oven temp. : 115 °C (hold 14 min.) to 180 °C at 20 °C/min): (*S*)-**4b** t_R = 12.8 min, (*R*)-**4b** t_R = 13.1 min. An analytically pure sample of **4b** had been previously obtained by flash chromatography on silica gel (cyclohexane / CH_2Cl_2: 100/0 → 85/15).[5] Colorless oil. For an enantiomeric ratio of 95:5 (*R*/*S*), $[\alpha]_D^{28}$ –59.4 (*c* = 0.98, CH_2Cl_2) (lit. [6a] er = 93:7 : $[\alpha]_D^{28}$ –50.6 (*c* = 0.97, CH_2Cl_2)).^{1}H NMR (400 MHz, $CDCl_3$) δ: 7.08–7.04 (m, 2H), 6.68 (td, *J* = 7.4, 0.9 Hz, 1H), 6.50 (d, *J* = 7.7 Hz, 1H), 5.90 (ddt, *J* = 17.2, 10.2, 6.0 Hz, 1H), 5.28 (app. dq, *J* = 17.2, 1.7 Hz, 1H), 5.18 (app. dq, *J* = 10.2, 1.7 Hz, 1H), 3.78 (app. ddt, *J* = 15.1, 6.0, 1.7 Hz, 1H), 3.61 (app. ddt, *J* = 15.1, 6.0, 1.7 Hz, 1H), 3.55 (app. t, *J* = 8.6 Hz, 1H), 3.28 (m, 1H), 2.85 (app. t, *J* = 8.6 Hz, 1H) 1.30 (d, *J* = 6.8 Hz, 3H). ^{13}C {^{1}H} NMR (100 MHz, $CDCl_3$) δ: 151.8, 135.2, 134.2, 127.4, 123.1, 117.7, 117.2, 107.3, 61.3, 52.0, 35.2, 18.6 (consistent with lit. [6a]).

Associated contents

The supporting information, including spectra of all new compounds, chiral stationary phase chromatograms and computed geometries and energies, is available free of charge on the ACS Publications website at :

Author information

Corresponding Authors

*E-mail : anne.boussonniere@univ-lemans.fr

*E-mail : anne-sophie.castanet@univ-lemans.fr

ORCID

Anne Boussonnière : 0000-0002-1113-099X

Anne-Sophie Castanet : 0000-0003-4704-4724

Notes

The authors declare no competing financial interest.

Acknowledgments

We gratefully acknowledge the French Ministry of Higher Education, Research and Innovation for H.G. PhD fellowship and the CNRS and Le Mans Université for financial support. We also thank Arnaud Martel for his help on the computational study and Rémi Busselez, Frédéric Legros, the NMR, mass spectroscopy and computation platforms for the technical support.

References and notes

1 a) Fañanás, F. J.; Sanz, R., Intramolecular carbolithiation reactions. In *The chemistry of organolithium compounds (2 parts)*, Rappoport, Z.; Marek, I., Eds. Wiley Interscience: Chichester, 2006; pp 295-379 ; b) Carl, E.; Stalke, D. Structure–Reactivity Relationship in Organolithium Compounds. In *Lithium Compounds in Organic Synthesis*; John Wiley & Sons, Ltd, 2014; pp 1–32 ; c) Gessner, V. H.; Däschlein, C.; Strohmann, C. Structure Formation Principles and Reactivity of Organolithium Compounds. *Chem. Eur. J.* **2009**, *15* (14), 3320–3334 ; d) Reich, H. J., Role of Organolithium Aggregates and Mixed Aggregates in Organolithium Mechanisms. *Chem. Rev.* **2013,** *113* (9), 7130-7178.

2 a) Hoppe, D.; Hense, T., Enantioselective Synthesis with Lithium/(−)-Sparteine Carbanion Pairs. *Angew. Chem. Int. Ed. Engl.* **1997,** *36* (21), 2282-2316 ; b) Hoppe, D.; Morgan, B. J.; Kozlowski, M. C., (−)-Sparteine. In *Encyclopedia of Reagents for Organic Synthesis*, 2007.

3 For **L1**-type ligands, see: a) Kizirian, J.-C., Chiral Tertiary Diamines in Asymmetric Synthesis. *Chem. Rev.* **2008,** *108* (1), 140-205 and references cited therein; b) Cabello, N.; Kizirian, J.-C.; Gille, S.; Alexakis, A.; Bernardinelli,

G.; Pinchard, L.; Caille, J.-C., Simple 1,2-Diamine Ligands for Asymmetric Addition of Aryllithium Reagents to Imines. *Eur. J. Org. Chem.* **2005,** (22), 4835-484; c) Steffen, P.; Unkelbach, C.; Christmann, M.; Hiller, W.; Strohmann, C., Catalytic and Stereoselective ortho-Lithiation of a Ferrocene Derivative. *Angew. Chem. Int. Ed.* **2013,** *52* (37), 9836-9840; d) Würthwein, E.-U.; Behrens, K.; Hoppe, D., Enantioselective Deprotonation of Alkyl Carbamates by Means of (*R*,*R*)-1,2-Bis(N,N-dimethylamino)cyclohexane/sec-Butyllithium— Theory and Experiment. *Chem. Eur. J.* **1999,** *5* (12), 3459-3463; e) Stead, D.; O'Brien, P.; Sanderson, A., A New Sparteine Surrogate for Asymmetric Deprotonation of N-Boc Pyrrolidine. *Org. Lett.* **2008,** *10* (7), 1409-1412; f) Metallinos, C.; Zaifman, J.; Dudding, T.; Van Belle, L.; Taban, K., Asymmetric Lithiation of Boron Trifluoride-Activated Aminoferrocenes: An Experimental and Computational Investigation. *Adv. Synth. Catal.* **2010,** *352* (11-12), 1967-1982; g) Praz, J.; Graff, J.; Egger, L.; Guénée, L.; Wagschal, S.; Kündig, E. P.; Alexakis, A. Asymmetric Bromine–Lithium Exchange: On the Importance of Both the Diamine Ligand and the Organolithium Reagent. *Chem. Commun.* **2015**, *51* (95), 16912–16915 and references cited therein.

4 For **L2** ligand, see: a) Hasegawa, M.; Taniyama, D.; Tomioka, K., Facile Asymmetric Synthesis of α-Amino Acids Employing Chiral Ligand-Mediated Asymmetric Addition Reactions of Phenyllithium with Imines. *Tetrahedron* **2000,** *56* (52), 10153-10158; b) Shindo, M.; Yamamoto, Y.; Yamada, K.-i.; Tomioka, K., Asymmetric Construction of Binaphthyl by the Chiral Diether-Mediated Conjugate Addition of Naphthyllithium to Naphthalenecarboxylic Acid 2,6-Di-*t*-butyl-4-methoxyphenyl Ester. *Chem. Pharm. Bull.* **2009,** *57* (7), 752-754 and references cited therein; c) Graff, J.; Łastawiecka, E.; Guénée, L.; Leroux, F.; Alexakis, A., Asymmetric Bromine–Lithium Exchange: Application toward the Synthesis of New Biaryl-Diphosphine Ligands. *Adv. Synth. Catal.* **2015,** *357* (13), 2833-2839; d) Nishimura, K.; Fukuyama, N.; Yamashita, M.; Sumiyoshi, T.; Yamamoto, Y.; Yamada, K.-i.; Tomioka, K., Cyclic Model for the Asymmetric Conjugate Addition of Organolithiums with Enoates. *Synthesis* **2015,** *47* (15), 2256-2264 and references cited therein.

5 Guyon, H.; Boussonnière, A.; Castanet, A.-S., Readily Accessible 1,2-Amino Ether Ligands for Enantioselective Intramolecular Carbolithiation. *J. Org. Chem.* **2017,** *82* (9), 4949-4957.

6 For articles on asymmetric intramolecular carbolithiation, see: a) Bailey, W. F.; Mealy, M. J., Asymmetric Cyclization of Achiral Olefinic Organolithiums Controlled by a Stereogenic Lithium: Intramolecular Carbolithiation in the Presence of (-)-Sparteine. *J. Am. Chem. Soc.* **2000,** *122* (28), 6787-6788; b) Sanz Gil, G.;

Groth, U. M., Enantioselective Synthesis of 3-Substituted Indolines by Asymmetric Intramolecular Carbolithiation in the Presence of (-)-Sparteine. *J. Am. Chem. Soc.* **2000,** *122* (28), 6789-6790; c) Barluenga, J.; Fañanás, F. J.; Sanz, R.; Marcos, C., Intramolecular carbolithiation of allyl o-lithioaryl ethers: A new enantioselective synthesis of functionalized 2,3-dihydrobenzofurans. *Chem. Eur. J.* **2005,** *11* (18), 5397-5407; d) Mealy, M. J.; Luderer, M. R.; Bailey, W. F.; Sommer, M. B., Effect of Ligand Structure on the Asymmetric Cyclization of Achiral Olefinic Organolithiums. *J. Org. Chem.* **2004,** *69* (18), 6042-6049; e) Groth, U.; Koettgen, P.; Langenbach, P.; Lindenmaier, A.; Schuetz, T.; Wiegand, M., Enantioselective synthesis of 3,3-disubstituted indolines via asymmetric intramolecular carbolithiation in the presence of (-)-sparteine. *Synlett* **2008,** (9), 1301-1304; f) Gómez-SanJuan, A.; Sotomayor, N.; Lete, E., Inter- and intramolecular enantioselective carbolithiation reactions. *Beilstein J. Org. Chem.* **2013,** *9*, 313-322.

7 Nguyen, T. T. T.; Guyon, H., Nguyen, K.P.P., Boussonnière, A.; Mortier, J.; Castanet, A.-S. Chiral Ligand-Mediated Nucleophilic Aromatic Substitution of Naphthoic Acids: A Fast and Efficient Access to Axially Chiral Biaryls. *Eur. J. Org. Chem.* **2020,** 10.1002/ejoc.202000317.

8 a) Mattalia, J.-M.; Nava, P., A Computational Study of the Intramolecular Carbolithiation of Aryllithiums: Solvent and Substituent Effects. *Eur. J. Org. Chem.* **2016,** (2), 394-401; b) Liu, S.; Gray, D.; Zhu, L.; Girolami, G. S., Lithium–Olefin π-Complexes and the Mechanism of Carbolithiation: Synthesis, Solution Behavior, and Crystal Structure of (2,2-Dimethylpent-4-en-1-yl)lithium. *Organometallics* **2019,** *38* (9), 2199-2210; c) Bailey, W. F.; Khanolkar, A. D.; Gavaskar, K.; Ovaska, T. V.; Rossi, K.; Thiel, Y.; Wiberg, K. B., Stereoselectivity of cyclization of substituted 5-hexen-1-yllithiums: regiospecific and highly stereoselective insertion of an unactivated alkene into a carbon-lithium bond. *J. Am. Chem. Soc.* **1991,** *113* (15), 5720-5727; d) Liu, H.; Deng, K.; Cohen, T.; Jordan, K. D., Computational Study of the Stereochemistry of Intramolecular Carbolithiation of an Alkene by a Secondary Alkyllithium: Stereochemistry Change Caused by a Single THF Molecule of Solvation. *Org. Lett.* **2007,** *9* (10), 1911-1914.

9 Grimme, S.; Antony, J.; Ehrlich, S.; Krieg, H., A consistent and accurate ab initio parametrization of density functional dispersion correction (DFT-D) for the 94 elements H-Pu. *The Journal of Chemical Physics* **2010,** *132* (15), 154104.

10 AIMAll (Version 15.09.27), Todd A. Keith, TK Gristmill Software, Overland Park KS, USA, 2017 (aim.tkgristmill.com).

11 The NCI analyses were conducted with the help of Multiwfn : Lu, T.; Chen, F., Multiwfn: A multifunctional wavefunction analyzer. *J. Comput. Chem.* **2012,** *33* (5), 580-592.

12 VMD was used for visualization of the NCI analyses: Humphrey, W.; Dalke, A.; Schulten, K., VMD: Visual molecular dynamics. *Journal of Molecular Graphics* **1996,** *14* (1), 33-38, http://www.ks.uiuc.edu/Research/vmd/.

13 Ross, G. A.; Koppang, M. D.; Bartak, D. E.; Woolsey, N. F. Cyclization of 2-(3-Butenyl)Bromobenzene via the Aryllithium Derivative. *J. Am. Chem. Soc.* **1985**, *107* (23), 6742–6743.

14 Whitesell, J. K., C_2 symmetry and asymmetric induction. *Chem. Rev.* **1989,** *89* (7), 1581-1590.

15 a) Humphries, A. C.; Pfaltz, A., Enantioselective Catalysis Using Sterically and Electronically Unsymmetrical Ligands. In *Stimulating Concepts in Chemistry*, 2000; pp 89-103; b) Pfaltz, A.; Drury, W. J., Design of chiral ligands for asymmetric catalysis: From C_2-symmetric P,P- and N,N-ligands to sterically and electronically nonsymmetrical P,N-ligands. *Proc. Natl. Acad. Sci. U.S.A.* **2004,** *101* (16), 5723-5726.

16 For a similar approach, see: Gessner, V. H.; Koller, S. G.; Strohmann, C.; Hogan, A.-M.; O'Shea, D. F., Mechanistic insight into stereoselective carbolithiation. *Chem. Eur. J.* **2011,** *17* (10), 2996-3004.

17 a) Lam, Y.-h.; Grayson, M. N.; Holland, M. C.; Simon, A.; Houk, K. N., Theory and Modeling of Asymmetric Catalytic Reactions. *Acc. Chem. Res.* **2016,** *49* (4), 750-762 ; b) Peng, Q.; Duarte, F.; Paton, R. S., Computing organic stereoselectivity – from concepts to quantitative calculations and predictions. *Chem. Soc. Rev.* **2016,** *45* (22), 6093-6107.

18 The SI includes cartesian coordinates of all the geometries of **2a**, **TS** and **3a** for ligands **L4a-c** and **L5a-c**.

19 a) Saito, Y., Absolute Configuration of Transition Metal Complexes. In *Stereochemistry of Optically Active Transition Metal Compounds*, American Chemical Society: 1980; Vol. 119, pp 13-42; b) Harris, S. E.; Pascual, I.; Orpen, A. G., Principal component analysis of conformations in fused ring chelate complexes: conformer identification, stereochemistry, and interconversion pathways. *J. Chem. Soc., Dalton Trans.* **2001,** (20), 2996-3009; c) Lucht, B. L.; Bernstein, M. P.; Remenar, J. F.; Collum, D. B., Polydentate Amine and Ether Solvates of Lithium Hexamethyldisilazide (LiHMDS): Relationship of Ligand Structure, Relative Solvation Energy, and

Aggregation State. *J. Am. Chem. Soc.* **1996,** *118* (44), 10707-10718; d) Ehnbom, A.; Ghosh, S. K.; Lewis, K. G.; Gladysz, J. A., Octahedral Werner complexes with substituted ethylenediamine ligands: a stereochemical primer for a historic series of compounds now emerging as a modern family of catalysts. *Chem. Soc. Rev.* **2016,** *45* (24), 6799-6811.

20 For greater clarity TS are represented without most of their hydrogens.

21 a) Desiraju, G. R.; Steiner, T., *The Weak Hydrogen Bond: In Structural Chemistry and Biology*. Oxford University Press: 2001. For reviews on non-classical C-H•••X bonding and their involvement in asymmetric processes, see: b) Johnston, R. C.; Cheong, P. H.-Y., C–H···O non-classical hydrogen bonding in the stereomechanics of organic transformations: theory and recognition. *Org. Biomol. Chem.* **2013,** *11* (31), 5057-5064; c) Ajitha, M. J.; Huang, K.-W., Non-Classical C-H···X Hydrogen Bonding and Its Role in Asymmetric Organocatalysis. *Synthesis* **2016,** *48* (20), 3449-3458.

22 a) Bader, R. F. W., *Atoms in Molecules: A Quantum Theory*. Clarendon Press: 1994; b) Matta, C. F.; Boyd, R. J.; Becke, A., *The Quantum Theory of Atoms in Molecules: From Solid State to DNA and Drug Design*. Wiley: 2007.

23 Koch, U.; Popelier, P. L. A., Characterization of C-H-O Hydrogen Bonds on the Basis of the Charge Density. *J. Phys. Chem.* **1995,** *99* (24), 9747-9754.

24 Heinl, T.; Retzow, S.; Hoppe, D.; Fraenkel, G.; Chow, A., Experimental and Theoretical Investigations of Lithio-Indenyl Carbamate/(−)-Sparteine and (−)-α-Isosparteine Complexes. *Chem. Eur. J.* **1999,** *5* (12), 3464-3470.

25 Only the parent transition state of **TS-L5c-λ-*R*Li-S_{C2}** with its OMe group in pseudo-axial position could be resolved and was 2 kcal/mol above **TS-L5c-δ-R_{Li}.S_{C2}**.

26 a) Seeman, J. I., Effect of conformational change on reactivity in organic chemistry. Evaluations, applications, and extensions of Curtin-Hammett Winstein-Holness kinetics. *Chem. Rev.* **1983,** *83* (2), 83-134; b) the assumption is made that diastereomeric complexes **2a** are interconverting rapidly in comparison to the carbolithiation kinetic.

27 For example, conversions determined by the ratio of indan **4a** and dehalogenated product arising from aryllithium **2a,** after the same reaction time (1h) were 89, 79 and 72 % for the diamine **L4a**, the amino ether **L4c** and the diether **L4b** respectively.

28 a) Bickelhaupt, F. M.; Houk, K. N., Analyzing Reaction Rates with the Distortion/Interaction-Activation Strain Model. *Angew. Chem. Int. Ed.* **2017,** *56* (34), 10070-10086; b) Fernández, I.; Bickelhaupt, F. M., The activation strain model and molecular orbital theory: understanding and designing chemical reactions. *Chem. Soc. Rev.* **2014,** *43* (14), 4953-4967; c) van Zeist, W.-J.; Bickelhaupt, F. M., The activation strain model of chemical reactivity. *Org. Biomol. Chem.* **2010,** *8* (14), 3118-3127; d) Alshakova, I. D.; Foy, H. C.; Dudding, T.; Nikonov, G. I. Ligand Effect in Alkali-Metal-Catalyzed Transfer Hydrogenation of Ketones. *Chem. – Eur. J.* **2019**, *25* (50), 11734–11744.

29 For the theory behind non-covalent interactions analysis, see: Johnson, E. R.; Keinan, S.; Mori-Sánchez, P.; Contreras-García, J.; Cohen, A. J.; Yang, W., Revealing Noncovalent Interactions. *J. Am. Chem. Soc.* **2010,** *132* (18), 6498-6506.

30 Salomone, A.; Perna, F. M.; Falcicchio, A.; Lill, S. O. N.; Moliterni, A.; Michel, R.; Florio, S.; Stalke, D.; Capriati, V. Direct Observation of a Lithiated Oxirane: A Synergistic Study Using Spectroscopic, Crystallographic, and Theoretical Methods on the Structure and Stereodynamics of Lithiated Ortho-Trifluoromethyl Styrene Oxide. *Chem. Sci.* **2014**, *5* (2), 528–538.

31 Reciprocally, a δ half-chair TS leading to the (S_{C2})-indan is enantiomeric and so energetically equal to the λ half-chair TS leading to the (R_{C2})-indan.

32 Burchat, A. F.; Chong, J. M.; Nielsen, N., Titration of alkyllithiums with a simple reagent to a blue endpoint. *J. Organomet. Chem.* **1997,** *542* (2), 281-283.

33 Watson, I. D. G.; Ritter, S.; Toste, F. D., Asymmetric Synthesis of Medium-Sized Rings by Intramolecular Au(I)-Catalyzed Cyclopropanation. *J. Am. Chem. Soc.* **2009,** *131* (6), 2056-2057.

34 Gotor-Fernández, V.; Fernández-Torres, P.; Gotor, V., Chemoenzymatic preparation of optically active secondary amines: a new efficient route to enantiomerically pure indolines. *Tetrahedron: Asymmetry* **2006,** *17* (17), 2558-2564.

35 Schanz, H.-J.; Linseis, M. A.; Gilheany, D. G., Improved resolution methods for (*R*,*R*)- and (*S*,*S*)-cyclohexane-1,2-diamine and (*R*)- and (*S*)-BINOL. *Tetrahedron: Asymmetry* **2003,** *14* (18), 2763-2769.

36 Chatterjee, A.; Sasikumar, M.; Joshi, N. N., Preparation of Enantiopure trans-1,2-Cyclohexanediol and trans-2-Aminocyclohexanol. *Synth. Commun.* **2007,** *37* (10), 1727-1733.

37 (1*S*,2*S*)-2-(methylamino)cyclohexanol is commercial or can be prepared by resolution of (±)-2-(methylamino)cyclohexanol with (*R*)-mandelic acid. Schiffers, I.; Rantanen, T.; Schmidt, F.; Bergmans, W.; Zani, L.; Bolm, C., Resolution of Racemic 2-Aminocyclohexanol Derivatives and Their Application as Ligands in Asymmetric Catalysis. *J. Org. Chem.* **2006,** *71* (6), 2320-2331.

38 Wang, Y.-M.; Bruno, N. C.; Placeres, Á. L.; Zhu, S.; Buchwald, S. L. Enantioselective Synthesis of Carbo- and Heterocycles through a CuH-Catalyzed Hydroalkylation Approach. *J. Am. Chem. Soc.* **2015**, *137* (33), 10524–10527.